



Physical-layer impairments estimation for random bandwidth traffic

Downloaded from: <https://research.chalmers.se>, 2026-04-10 23:36 UTC

Citation for the original published paper (version of record):

Xu, Y., Agrell, E., Brandt-Pearce, M. (2024). Physical-layer impairments estimation for random bandwidth traffic. *Journal of Optical Communications and Networking*, 16(2): 104-111.
<http://dx.doi.org/10.1364/JOCN.506424>

N.B. When citing this work, cite the original published paper.

© 2024 IEEE. Personal use of this material is permitted. Permission from IEEE must be obtained for all other uses, in any current or future media, including reprinting/republishing this material for advertising or promotional purposes, or reuse of any copyrighted component of this work in other works.

Physical-Layer Impairments Estimation for Random Bandwidth Traffic

YUXIN XU¹, ERIK AGRELL², AND MAITE BRANDT-PEARCE^{3,*}

¹College of Information Engineering, Zhejiang University of Technology, Hangzhou, Zhejiang, China, 310000.

²Department of Electrical Engineering, Chalmers University of Technology, SE-41296 Gothenburg, Sweden.

³Charles L. Brown Department of Electrical and Computer Engineering, University of Virginia, Charlottesville, Virginia 22904, USA.

*mb-p@virginia.edu

Compiled December 19, 2023

Traffic demands in future elastic optical networks are expected to be heterogeneous with time-varying bandwidth. Estimating the physical-layer impairments (PLIs) for random bandwidth demands is important for cross-layer network resource provisioning. State-of-the-art PLI estimation techniques yield conservative PLI estimates using the maximum bandwidth, which leads to significant over-provisioning. This paper uses probabilistic information on random bandwidth demands to provide a computationally efficient, accurate, and flexible PLI estimate. The proposed model is consistent with the needs of future self-configuring fiber-optic networks and maximally avoids up to a 25% overestimation of PLIs compared to the benchmark for the cases studied, thus reducing the network design margin at a negligible extra computational cost.

<http://dx.doi.org/10.1364/ao.XX.XXXXXX>

1. INTRODUCTION

Elastic optical networks (EONs) have been considered a potential solution to meet society's increasing requirements for future communication networks [1]. The near future may include self-configuring EONs [2, 3], which rely on a feedback scheme in order to configure networks according to the current network state, thereby providing lower design margins while using efficient resource management [4]. In these networks, the traffic will need to be estimated and predicted as statistical information using probabilistic modeling. While signals traverse long-haul fiber-optic networks, their quality is impaired because of the accumulated noise and interference, jointly called physical layer impairments (PLIs) [5]. Considering the PLIs is essential in network planning and resource allocation because they directly impact the quality of transmission (QoT) of optical signals. This paper proposes an analytic model to estimate the PLIs statistically for time-varying traffic with randomly varying bandwidth [6, 7]. The resulting PLI estimate has a predictable performance without resorting to over-conservative, worst-case assumptions.

Because of the large number of data transmissions and the variability of human activity, the demand volume across time and space can vary significantly. The requested data-rates can change due to many factors such as time, weather, major events, etc. [8, 9]. However, current network infrastructure and configurations (such as regeneration sites and switches) are typically pre-defined; conventional fiber-optic networks cannot reconfigure resources in response to time-varying traffic. In order to

handle changes in a connection's data-rate, one of two methods can be used: 1) change the modulation format and keep the bandwidth unchanged. 2) change the bandwidth. For the first method, when a high modulation format is chosen to address an increase in the data-rate, there is an increase in the required signal-to-noise ratio (SNR), which shortens the allowed signal transmission distances; this can result in the need for expensive regeneration circuits for long-reach traffic. The second option, which allows the bandwidth to vary, becomes appealing [8]. This would result in a traffic model based on the probability distribution of the signal bandwidths.

The currently used approaches to PLI estimation provide accurate and state-dependent estimates in the steady-state, without accounting for random or time-varying traffic parameters. Many detailed models of the PLIs have been developed for signal-level analysis [10–14]; these multi-integral expressions can be extremely accurate but are far too complex to use as part of a real-time network management task. The so-called Gaussian noise (GN) model provides simple closed-form expressions of the self-interference and cross-channel interference [15–17]. Many extensions to the GN model have been proposed to improve its accuracy and applicability [17–19], but none is immediately usable when the given demands are time-varying with random bandwidth. The *statistical network assignment process* (SNAP) algorithm based on Monte Carlo simulations to estimate the PLIs of random bandwidth demands has been proposed recently [20, 21]. It provides a highly accurate PLI estimate when many simulation trials are used; this can be computationally demanding, making SNAP more attractive for use in off-line

network resource provisioning than for real-time dynamic resource allocation. In state-of-the-art network resource allocation schemes, time-varying demands are typically accommodated by using their maximum anticipated bandwidth in the GN model. This PLI estimate, which we refer to as the *maximum bandwidth GN model*, can result in network resources being severely over-provisioned and thus wastes scarce network resources when the traffic bandwidth is highly variable [20–22].

The *probabilistic spectrum Gaussian noise* (PSGN) model, first proposed in [6], can estimate the PLIs for random bandwidth demands in EONs operating over the C-band based on the statistics of the PLI, resulting in a somewhat conservative estimate. It derives simple expressions for the expected value and variance of the self-channel interference (SCI) and the expected value of the cross-channel interference (XCI) given the probability density function (PDF) of the demand's bandwidth. The PSGN model showed significant improvement in performance and complexity compared to the SNAP algorithm [6, 7].

In this paper, we derive probabilistic expressions for the PLI, refine the PSGN model to include the variance of the XCI, and show how these expressions can be combined in a PLI estimate with a given degree of reliability. This is achieved using the outage probability for the PLI based on the derived probability distributions. The outage probability of a noise estimation model represents the probability that the actual noise level exceeds the estimated noise level, and typically ranges from 2% to 10%. It is a specification that balances the model robustness and design margin savings. The PSGN model with a guaranteed outage probability can be used to link the prediction of the traffic and estimation of the corresponding PLIs needed in self-configuring networks.

This paper is organized as follows. In Section 2, we present the PSGN model and derive the outage probability for uniformly distributed traffic bandwidths. In Section 3, simulation settings and numerical results are given and discussed. We draw conclusions and describe opportunities for expanding on the proposed approach in Section 4.

2. PROBABILISTIC SPECTRUM GAUSSIAN NOISE MODEL

In this section, we introduce our PSGN PLI model for traffic with randomly defined bandwidth. We start with the conventional GN model, describe the SNAP algorithm used for comparison, and then derive the PSGN model mathematically. Lastly, we present an analytic expression of the outage probability of the PSGN model.

In continental-scale optical networks, we consider two main types of PLIs: amplified spontaneous emission (ASE) noise and nonlinear interference (NLI) noise caused by the interaction of Kerr fiber nonlinearity and chromatic dispersion. In this work, only C-band transmission is considered, and, therefore, inter-channel stimulated Raman scattering is assumed negligible [10, 12].

EDFAs are used as signal amplifiers at the end of each span to compensate for the transmission loss [16, 23]. Because modern EDFAs are designed to have an almost flat gain over the whole C-band, we assume the gain of the EDFA is flat in this work, as is common in the literature [24, 25]. The optical amplification process adds ASE noise, which in this case can be modeled as additive Gaussian noise with constant power spectral density

(PSD) per polarization in one span given as [16]

$$G_{\text{ASE}} = (e^{\alpha L} - 1)h\nu n_{\text{sp}}, \quad (1)$$

where h is Planck's constant, n_{sp} is the spontaneous emission factor, α is the fiber power attenuation, ν is the light frequency, and L is the fiber length per span. As is typically assumed [26], one EDFA exactly compensates for the loss in one fiber span. Based on our assumptions, the PSD of the ASE noise depends only on the transmission length and not the signal bandwidth, and thus, we omit it from our probabilistic model; the constant ASE noise added in each span can be accounted for in the final calculation of the SNR.

A. Gaussian Noise Model

The GN model is used to analytically estimate the NLI PSD, and is valid for systems adhering to the following main assumptions [15, 16, 26]: the fiber links are dispersion uncompensated; each signal has rectangular PSD, which is the same in both polarizations; the fiber loss is totally compensated; the NLI PSD is accumulated along the lightpath; and the multi-channel interference can be neglected.

The NLI effects for each span can be divided into self-channel interference (SCI) and cross-channel interference (XCI),

$$G_{\text{NLI}} = G_{\text{SCI}} + \sum_{q=1, q \neq p}^{M_c+1} G_{\text{XCI},q}, \quad (2)$$

where G_{NLI} represents the channel of interest's NLI PSD per span, G_{SCI} represents the SCI PSD, and $G_{\text{XCI},q}$ represents the contribution to the XCI PSD due to the q th interfering channel. M_c represents the number of channels sharing the fiber span with the channel of interest, denoted as channel p .

SCI is caused by channel p itself, only varying with the bandwidth Δ_p of the channel as

$$G_{\text{SCI}}(\Delta_p) = \mu G_p^3 \operatorname{arcsinh}(\rho \Delta_p^2), \quad (3)$$

where G_p is the signal PSD of the channel of interest, $\rho = (\pi^2 |\beta_2|) / 2\alpha$, $\mu = (3\gamma^2) / (2\pi\alpha |\beta_2|)$, γ denotes the fiber nonlinearity parameter, and β_2 denotes the group velocity dispersion parameter. When Δ_p is large ($\Delta_p^2 \gg 2\alpha / (\pi^2 |\beta_2|)$), the inverse hyperbolic sine function and the logarithm function are similar. Equation (3) can thus be replaced by [15]

$$G_{\text{SCI}}(\Delta_p) = \mu G_p^3 \ln(\rho \Delta_p^2). \quad (4)$$

The XCI is caused by the interaction between channels. It depends on the center frequency differences and bandwidths of neighboring channels sharing the same fiber link with the channel of interest p . The PSD of the XCI on channel p caused by the presence of channel q , $q \neq p$, can be written as

$$G_{\text{XCI},q}(\Delta_q) = \mu G_p G_q^2 \ln \left(\frac{|f_p - f_q| + \Delta_q/2}{|f_p - f_q| - \Delta_q/2} \right), \quad (5)$$

where f_q represents the center frequency of channel q and G_q is the signal PSD in channel q .

When the actual signal bandwidths are not known, the GN model typically upper-bounds the NLI per span by using the maximum of the random bandwidth over all realizations, resulting in

$$G^{\text{GN}} = G_{\text{SCI}}(\max \Delta_p) + \sum_{q=1, q \neq p}^{M_c+1} G_{\text{XCI},q}(\max \Delta_q), \quad (6)$$

which we refer to as the *maximum bandwidth GN model*. G^{GN} is a conservative estimate of the NLI for random bandwidth demands.

B. SNAP algorithm

The statistical network assignment process (SNAP) algorithm is a Monte Carlo based PLI estimate for time-varying bandwidth demands. It utilizes the GN model implemented in the GNPY library to estimate the PLIs needed to compute the SNR for the assigned lightpath at each Monte Carlo trial [20]. Figure 1 in [20] shows a flow-chart of the SNAP algorithm. The algorithm requires numerous Monte Carlo trials to comprehensively simulate the many network states and obtain a statistical assessment of the network used to compute the demand blocking probability.

C. PSGN Model

Given the traffic model, the statistics of the random bandwidth demands can be used to develop a probabilistic NLI model, which we refer to as the PSGN model. In this section, we derive analytical expressions for the noise statistics to create the PSGN model. Again, we assume that the NLI accumulates incoherently over all spans of the transparent fiber segment.

Both the PSGN model and the SNAP algorithm use the GN model to estimate the NLI caused by traffic with random bandwidth. Unlike the SNAP algorithm, the PSGN model does not require many trials of Monte Carlo simulations. It instead derives the statistics analytically. Therefore, compared with the SNAP algorithm, the PSGN model is just as accurate at estimating the NLI but much more computationally efficient.

In our derivation, for notational simplicity we assume that the signal of interest is centered at frequency $f_p = 0$ (without loss of generality). For each demand q sharing the same link with the channel of interest p , we assume that the bandwidth PDF is known and denoted as $f_{\Delta_q}(\delta)$. The cumulative density function (CDF) is denoted by $F_{\Delta_q}(\delta)$. Δ_q is the random variable representing the bandwidth of demand q with realization $\delta \in [\delta_{\min,q}, \delta_{\max,q}]$.

The SCI for the channel of interest depends primarily on its own bandwidth. The expected SCI noise becomes

$$\begin{aligned} E[G_{\text{SCI}}] &= \mu G_p^3 E \left[\ln(\rho \Delta_p^2) \right] \\ &= \mu G_p^3 \int_0^\infty \ln(\rho \delta^2) f_{\Delta_p}(\delta) d\delta, \end{aligned} \quad (7)$$

and its variance is

$$\text{Var}[G_{\text{SCI}}] = \mu^2 G_p^6 \int_0^\infty \ln^2(\rho \delta^2) f_{\Delta_p}(\delta) d\delta - E^2[G_{\text{SCI}}]. \quad (8)$$

These integrals can be solved exactly for a uniformly distributed bandwidth demand as done in Section 3, but in general must be computed numerically.

Using (5), the expected XCI contributed by demand q with bandwidth Δ_q to the channel of interest p is

$$\begin{aligned} E[G_{\text{XCI},q}] &= \mu G_p G_q^2 E \left[\ln \left(\frac{|f_q| + \delta/2}{|f_q| - \delta/2} \right) \right] \\ &= \mu G_p G_q^2 \int_0^\infty \ln \left(\frac{|f_q| + \delta/2}{|f_q| - \delta/2} \right) f_{\Delta_q}(\delta) d\delta. \end{aligned} \quad (9)$$

We apply integration by parts to obtain

$$\begin{aligned} E[G_{\text{XCI},q}] &= \frac{\mu G_p G_q^2}{2} \left\{ \int_{\delta_{\min,q}}^{\delta_{\max,q}} \left[\frac{1}{|f_q| - \delta/2} \right] \cdot [1 - F_{\Delta_q}(\delta)] d\delta \right. \\ &\quad \left. + \int_{\delta_{\min,q}}^{\delta_{\max,q}} \left[\frac{1}{|f_q| + \delta/2} \right] \cdot [1 - F_{\Delta_q}(\delta)] d\delta \right\}. \end{aligned} \quad (10)$$

Given that the center frequency $|f_q| > \delta_{\max,q}/2$ is the same for every realization δ of demand q , and substituting $\delta = 2(|f_q| - f)$ for the first integral in (10) and $\delta = 2(f - |f_q|)$ for the second, the expected XCI contributed by channel q can be simplified as

$$E[G_{\text{XCI},q}] = \mu G_p G_q^2 \int_{\delta_{\min,q} \leq 2|f - |f_q|| \leq \delta_{\max,q}} \frac{1 - F_{\Delta_q}(2|f - |f_q||)}{f} df. \quad (11)$$

The same method used to derive (11) can unfortunately not be used to simplify the expression for the variance of the XCI, which must be computed directly as

$$\begin{aligned} \text{Var}[G_{\text{XCI},q}(\delta)] & \\ &= \mu^2 G_p^2 G_q^4 \int_0^\infty \ln^2 \left(\frac{|f_q| + \delta/2}{|f_q| - \delta/2} \right) f_{\Delta_q}(\delta) d\delta - E^2[G_{\text{XCI},q}]. \end{aligned} \quad (12)$$

The proposed PSGN model provides a conservative estimate of the NLI noise based on a user-set parameter r . The PSGN PSD is defined as

$$\begin{aligned} G^{\text{PSGN}} &= E[G_{\text{SCI}}] + \sum_{q, q \neq p} E[G_{\text{XCI},q}] \\ &+ r \left(\sqrt{\text{Var}[G_{\text{SCI}}]} + \sqrt{\sum_{q, q \neq p} \text{Var}[G_{\text{XCI},q}]} \right). \end{aligned} \quad (13)$$

When $r = 0$, the PSGN model gives the expected value of the total signal nonlinear interference. The model is more conservative when r increases, and thus the robustness of the whole system increases. The estimate might be over-conservative with a larger value for r , which leads to over-provisioning and resource wastage. The term $\sqrt{\sum_{q, q \neq p} \text{Var}[G_{\text{XCI},q}]}$ (ignored in [6]) varies with the number and the bandwidths of neighboring channels. The term is smaller than $\sqrt{\text{Var}[G_{\text{SCI}}]}$ but still important to consider. For example, when two neighboring channels, uniformly distributed from 50 to 100 GHz and with maximum bandwidths separated by 12.5 GHz, were tested, the contribution from the XCI variance was found to be 13.4% of the contribution from the SCI variance.

In modern optical network design and control mechanisms [2, 4], different network models have various reliability requirements. There is a trade-off between network design margins and reliability. Low-margin networks, such as advanced autonomous networks, can dynamically adjust the network configuration, including routing and modulation formats. Therefore, a controllable NLI estimation model can provide more flexibility for network operators adapting to different scenarios and providing various customized network services [4].

Note that the proposed PSGN method could account for other impairments as long as a mathematical relation between the PSD of the noise due to the impairment and the bandwidth of the signal is known.

D. PSGN Outage Probability

The PSGN outage probability measures the probability that the actual NLI generated by random bandwidth demands exceeds the NLI PSD estimated by the PSGN model in (13). It measures the reliability and robustness of the PSGN model. Thus, the outage probability strongly relates to the parameter r . In our previous work [6], the outage probability was calculated by Monte Carlo simulation, i.e., for each trial we randomly selected a bandwidth according to the demand's probability distribution and then calculated the probability that the simulated NLI exceeds the PSGN model. In this work, we derive expressions for the outage probability using NLI equations for one fiber span; if we consider several spans carrying the same traffic on a fiber link, the outage probability is the same as for the single span case.

We derive an analytic model for the outage probability under the assumption that all bandwidths are uniformly distributed over a known range, which is a common assumption [20, 22, 27]. The technique can be applied to any analytically or numerically defined bandwidth PDF. An analytical outage model makes the PSGN model easier to apply to various situations. For example, a network designer can use the PSGN model to analyze system-wide design margins with a low computational cost. The results calculated by the analytic outage probability model are also more accurate compared to when they are obtained via Monte Carlo simulations.

Obtaining the PSGN outage probability requires deriving the PDF of the NLI for the channel of interest p . The CDF of the PSD for the channel of interest's SCI can be derived from (4) as

$$F_{G_{\text{SCI}}}(x) = \Pr \left[\mu G_p^3 \ln(\rho \Delta_p^2) \leq x \right] = F_{\Delta_p} \left(\sqrt{\exp(x/\mu G_p^3)/\rho} \right). \quad (14)$$

When Δ_p , the random bandwidth of demand p , is uniformly distributed within $[\delta_{\min,p}, \delta_{\max,p}]$, we can write

$$F_{G_{\text{SCI}}}(x) = \begin{cases} 0 & x \leq \mu G_p^3 \ln(\delta_{\min,p}^2/\rho) \\ 1 & x > \mu G_p^3 \ln(\delta_{\max,p}^2/\rho) \\ \frac{\sqrt{\exp(x/\mu G_p^3)/\rho} - \delta_{\min,p}}{\delta_{\max,p} - \delta_{\min,p}} & \Pi_{\text{SCI}}(x), \end{cases} \quad (15)$$

where

$$\Pi_{\text{SCI}}(x) = \{x | x \in [\mu G_p^3 \ln(\delta_{\min,p}^2/\rho), \mu G_p^3 \ln(\delta_{\max,p}^2/\rho)]\}. \quad (16)$$

Thus, defining the rectangular function $\text{rect}_A(a) = 1$ for $a \in A$ and zero elsewhere, the PDF of the SCI PSD for the channel of interest p is

$$f_{G_{\text{SCI}}}(x) = \frac{\exp(x/2\mu G_p^3) \text{rect}_{\Pi_{\text{SCI}}}(x)}{2\mu G_p^3 \sqrt{\rho} (\delta_{\max,p} - \delta_{\min,p})}. \quad (17)$$

Similarly, the CDF of the XCI PSD contributed by channel q onto channel p can be derived from (5) as

$$F_{G_{\text{XCI},q}}(x) = \Pr \left[G_{\text{XCI},q} \leq x \right] = F_{\Delta_q} \left(\frac{2|f_q| \left[\exp(x/\mu G_p G_q^2) - 1 \right]}{\exp(x/\mu G_p G_q^2) + 1} \right). \quad (18)$$

Under the same assumptions as above, the CDF becomes

$$F_{G_{\text{XCI},q}}(x) = \left[\frac{2|f_q| \left[\exp(x/\mu G_p G_q^2) - 1 \right]}{\exp(x/\mu G_p G_q^2) + 1} - \delta_{\min,q} \right] \frac{1}{\delta_{\max,q} - \delta_{\min,q}}, \quad (19)$$

for

$$\Pi_{\text{XCI},q}(x) = \left\{ x \mid x \in \left[\mu G_p G_q^2 \ln \left(\frac{|f_q| + \delta_{\min,q}/2}{|f_q| - \delta_{\min,q}/2} \right), \mu G_p G_q^2 \ln \left(\frac{|f_q| + \delta_{\max,q}/2}{|f_q| - \delta_{\max,q}/2} \right) \right] \right\}. \quad (20)$$

Therefore, the PDF of the XCI PSD is

$$f_{G_{\text{XCI},q}}(x) = \frac{4|f_q| \exp(x/\mu G_p G_q^2) / \mu G_p G_q^2 \text{rect}_{\Pi_{\text{XCI},q}}(x)}{[\exp(x/\mu G_p G_q^2) + 1]^2 (\delta_{\max,q} - \delta_{\min,q})}. \quad (21)$$

The PSD of the NLI terms is additive, as shown in (2). Assuming that the SCI and XCI are independent and that the XCI contributed by different channels are also independent, if all channels have uniformly distributed bandwidths, we obtain an expression for the PDF of the NLI as

$$f_{G_{\text{NLI}}}(x) = f_{G_{\text{SCI}}}(x) * f_{G_{\text{XCI},1}}(x) * \dots * f_{G_{\text{XCI},p-1}}(x) * f_{G_{\text{XCI},p+1}}(x) * \dots * f_{G_{\text{XCI},M_c+1}}(x) = \frac{\exp(x/2\mu G_p^3) \text{rect}_{\Pi_{\text{SCI}}}(x)}{2\mu G_p^3 \sqrt{\rho} (\delta_{\max,p} - \delta_{\min,p})} * \dots * \left[\frac{4f_{M_c+1} \exp(x/\mu G_p G_q^2) / \mu G_p G_q^2 \text{rect}_{\Pi_{\text{XCI},M_c+1}}(x)}{[\exp(x/\mu G_p G_q^2) + 1]^2 (\delta_{\max,M_c+1} - \delta_{\min,M_c+1})} \right], \quad (22)$$

where $*$ denotes convolution. Note that if an operator has statistical data on their network traffic, they can apply this approach to the histogram of traffic bandwidth data numerically.

The outage probability \mathcal{P} , defined as the probability that the actual noise exceeds the estimated noise G^{PSGN} , is then

$$\mathcal{P} = 1 - F_{G_{\text{NLI}}}(G^{\text{PSGN}}) = \int_{G^{\text{PSGN}}}^{\infty} f_{G_{\text{NLI}}}(x) dx. \quad (23)$$

Hence, if a network designer aims to satisfy a given outage probability \mathcal{P} , such as 2% or 5%, the \mathcal{P} -outage NLI estimate G_p needs to be found using $F_{G_{\text{NLI}}}(G_p) = 1 - \mathcal{P}$. The parameter r , which controls how conservative the PSGN estimate is, can be mathematically determined via (13) to yield the desired outage \mathcal{P} using

$$r = \frac{G_p - E[G_{\text{SCI}}] - \sum_q E[G_{\text{XCI},q}]}{\sqrt{\text{Var}[G_{\text{SCI}}] + \sum_{q,q \neq p} \text{Var}[G_{\text{XCI},q}]}}. \quad (24)$$

3. NUMERICAL RESULTS

In this section, we estimate the span-level NLI in an EON using the proposed PSGN model, compared with the benchmark, the maximum bandwidth GN model. The maximum bandwidth GN model (6), denoted as G^{GN} , uses the maximum bandwidth of random bandwidth demands to estimate the NLI in order to guarantee the signal QoT. The system parameters used in our numerical results are listed in Table 1. The guard band between neighboring channels is defined as the frequency spacing

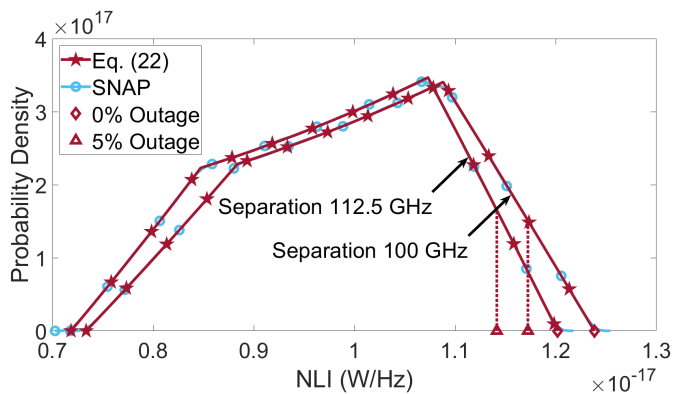
Table 1. System Parameters [15]

β_2	$-21.7 \text{ ps}^2/\text{km}$
$G_p = G_q$	0.015 W/THz
γ	$1.32 \times 10^{-3} (\text{W} \cdot \text{m})^{-1}$
Span length	100 km
n_{sp}	1.58
α	0.22 dB/km
ν	193.55 THz
Guard band	12.5 GHz
Fiber type	standard single mode fiber

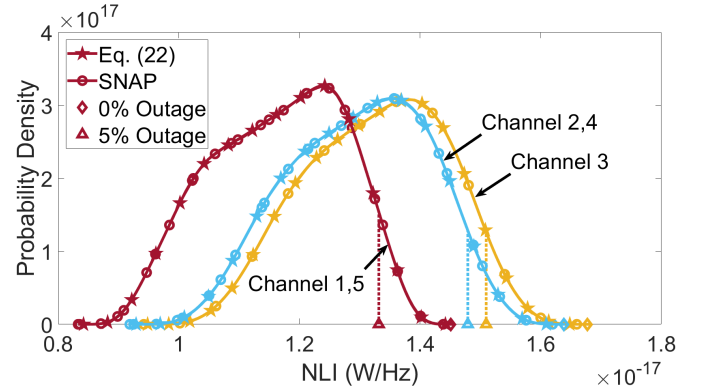
between the maximum signal bandwidths. To simplify the computation and be consistent with modern optical network settings, G_p is set to be equal to G_q [28].

Figs. 1 and 2 provide results to verify the accuracy of the derivation of the NLI PDF for two and five channels, respectively. One span of standard single mode fiber is tested. We use the SNAP method as the benchmark, where all demand bandwidths are randomly selected according to a uniform distribution and applied to each trial of a Monte Carlo simulation. SNAP has been used before to model random traffic [20–22]. Eq. (22) is evaluated numerically using nested integrals, i.e., cascaded convolution, which is computationally simple for uniformly distributed random bandwidth demands; we compare the computational complexity of the various methods in Fig. 4, discussed below. The NLI PDF obtained by (22) is consistent with the kernel density estimate [29, 30] obtained from the Monte Carlo simulation results with 10^8 trials. Both the expected value and variance calculated using (22) have less than a 0.01% difference compared to the results obtained by the Monte Carlo simulation.

In Fig. 1, two channels transmitted through one span have random bandwidths distributed from 50 to 100 GHz, and two channel separations are tested, 100 and 112.5 GHz, corresponding to guard bands of 0 and 12.5 GHz, respectively. The NLI estimate corresponding to a $\mathcal{P} = 5\%$ outage, $G_{5\%} = 1.13 \times 10^{-17}$ W/Hz for a separation of 112.5 GHz and $G_{5\%} = 1.17 \times 10^{-17}$ W/Hz for a separation of 100 GHz, are marked with triangle symbols. The G^{GN} estimate is also shown with a diamond symbol at the right-most end of the NLI PDF curve; note that $G^{\text{GN}} = G_{\mathcal{P}}$ for $\mathcal{P} = 0\%$ outage probability.

**Fig. 1.** NLI PDF $f_{G^{\text{NLI}}}$ for the channel of interest with one interfering channel, $M_c = 1$.

In Fig. 2, five channels with bandwidths uniformly distributed from 50 to 100 GHz and successively numbered as channel 1 through channel 5, are transmitted on the same fiber span. In this and subsequent results, guard bands of 12.5 GHz separate the channels' maximum bandwidths. For each curve, one channel is considered the channel of interest placed at $f_p = 0$, as assumed in (22), and the other four channels are considered interferers in order to verify the proposed analytic model; for example, when the interference affecting channel $p = 2$ is studied, the channels have center frequencies $(f_1, \dots, f_5) = (-112.5, 0, 112.5, 225, 337.5)$ GHz. Recall that only center frequency differences between the interferers and the channel of interest matter for NLI. Channel 3 is sandwiched in the middle of the spectrum and thus experiences the highest NLI when selected as the channel of interest. Channels 2 and 4 have similar NLI, greater than the NLI seen by channels 1 and 5. The shapes of the NLI PDFs are similar, as expected. Compared with the two-channel scenario in Fig. 1, the NLI PDFs for five channels have longer tails, which means that G^{GN} is larger and farther away from $G_{5\%}$, again marked in the figure with diamonds and triangles, respectively.

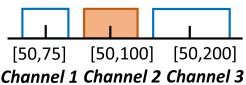
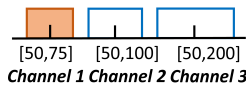
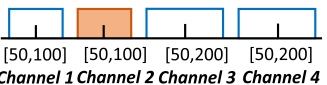
**Fig. 2.** NLI PDFs $f_{G^{\text{NLI}}}$ for five channels transmitting on the same fiber link, $M_c = 4$.

The value of r in the PSGN model resulting in a desired outage probability $\mathcal{P} = 0\%, 0.25\%, 1\%, 2\%$, and 5% is shown in Figs. 3 (a) and (b) as a function of the number of homogeneous channels on the span with bandwidths uniformly distributed in $[50, 100]$ GHz and $[50, 200]$ GHz, respectively; note that the number of channels on the x-axis includes the channel of interest. When the number of channels increases, r estimated by (24) decreases for any fixed outage probability \mathcal{P} greater than 1%. However, the estimated r for outage probability less than 1%, including $\mathcal{P} = 0\%$ (leading to G^{GN}), increases as the number of channels increases. Therefore, for $\mathcal{P} > 1\%$ the PSGN model with a value for r that gives a desired outage probability for two channels guarantees that the outage probability is also satisfied when more channels share the link.¹ In subsequent results, we refer to this r as the *guaranteed* r , and the r that gives an exact outage probability as the *exact* r .

Table 2 shows the impact of parameter r for heterogeneous traffic. Several heterogeneous traffic scenarios are considered, showing the values of the exact r and the resulting PSGN NLI estimate for the shaded channel when a subset of channels is

¹It is difficult to state what value of outage probability is acceptable for any particular optical network as this paper is the first to propose this performance metric. An outage, however, will cause a traffic request to be blocked, and blocking probabilities of 1% to 5% are commonly cited in the literature [31, 32].

Table 2. Impact of Parameter r

Guard band = 12.5 GHz	Channels	Exact r			$G^{\text{PSGN}} (\times 10^{-17})$ W/Hz		
		5%	2%	0%	5%	2%	0%
 Channel 1 Channel 2 Channel 3	1, 2	1.317	1.406	1.542	1.188	1.202	1.227
	2, 3	1.149	1.321	1.609	1.168	1.184	1.231
	1, 2, 3	1.155	1.319	1.701	1.167	1.184	1.247
 Channel 1 Channel 2 Channel 3	1, 2	1.240	1.375	1.608	0.946	0.962	0.994
	1, 2, 3	1.174	1.351	1.855	0.941	0.964	1.003
 Channel 1 Channel 2 Channel 3 Channel 4	1, 2	1.255	1.370	1.571	1.265	1.284	1.308
	2, 3	1.160	1.325	1.624	1.244	1.280	1.312
	1, 2, 3, 4	1.145	1.324	1.968	1.242	1.280	1.376

considered. Three scenarios are depicted, and in each case a subset of the channels shown, as indicated in the column labeled *Channels*, is accounted for in the computation. In the figures embedded in the first column, each channel has a bandwidth in GHz uniformly distributed in the interval indicated below each spectrum. G^{PSGN} represents the NLI estimated by (13) using the corresponding exact r .

Table 2 further evidences our conclusion from Fig. 3 that determining the guaranteed r only requires considering the channel of interest and the one neighboring channel that causes the most XCI when the desired outage probability is larger than 1%. As expected from Fig. 3, the exact r is smaller when considering three or four channels than when only considering one neighboring channel. Thus, instead of performing M_c cascaded convolutions, (22) can be simplified to the convolution of just two PDFs to obtain the guaranteed r using (24), and then (13) is used to obtain the G^{PSGN} estimate of the NLI. Using the guaranteed r in the PSGN model saves significant computation time while still ensuring the desired outage.

Fig. 4 shows the computational advantage of using the PSGN model with the guaranteed r compared with other approaches. The computational cost of an algorithm is captured by the elapsed computation time needed to obtain the result.² The state-of-the-art SNAP algorithm described above, which uses Monte Carlo simulations, is used as a benchmark. It requires almost 1000 s to estimate the NLI for the channel of interest when 13 channels share the fiber link. Limiting the number of channels sharing each link to 13 guarantees that the transmission on each lightpath within the network will not exceed C-band. For the same scenario, the PSGN model with the exact r obtains the same result but only requires 471 s, saving 52% of the computation time. The PSGN model with the guaranteed r , obtained by assuming only the channel of interest and one of its closest neighbors, requires even less, 194 s. In some situations, the PSGN model could use a known value for r from a previous empirical result (labeled ‘PSGN Empirical r ’ in the figure legend), shrinking the time needed to estimate the NLI down to a fraction of a second. The GN model is significantly faster than the PSGN Empirical r , but they both require less than 30 ms per estimation. The PSGN model is sufficiently fast for

most applications.

The advantage of using the PSGN model to estimate the NLI over the overly-conservative maximum bandwidth GN model, G^{GN} , is shown in Fig. 5. For a channel of interest with uniformly distributed bandwidth ranging from 50 to 100 GHz, the NLI estimated by the PSGN model with an outage probability of 5% can avoid up to 10% of NLI overestimation. For demands with bandwidths uniformly distributed from 50 to 200 GHz, the GN model overestimates the NLI by 16% compared to the NLI estimated by the PSGN model, at the cost of 2% outage probability. The proposed PSGN model can avoid up to 25% of NLI overestimation for a span with 13 signals with highly variable bandwidths and 5% outage. Note that this NLI saving is just for the channel of interest.

4. CONCLUSIONS

The proposed PSGN model estimates the NLI for random bandwidth demands. It is applied to guarantee the QoT with a chosen outage probability and requires only the channel of interest and one neighboring channel. Compared to the GN model, the PSGN model avoids significant NLI overestimation without incurring an excessive computational burden.

Optical network planners use design margins to guarantee a desired performance, but these margins use valuable resources [2]. The proposed PSGN model is simple enough to be utilized in cross-layer resource management of continental-scale optical networks to significantly reduce these margins. The PSGN model is applicable to future communication scenarios with heterogeneous and time-varying traffic where statistical information for the traffic is known. Thus, it could be used in self-configuring networks to guarantee the QoT after reconfiguration [6, 33]. Studying the benefits of using the PSGN model in self-configuring networks is the subject of future research.

In the numerical results of this work, the channel powers are assumed to be equal. The proposed PSGN model works with any launch power scheme. Therefore, the effect of signal launch power of random bandwidth traffic (including power optimization) and the resulting accumulated PLI distributions are also of interest and the subject of future studies.

Funding. National US NSF under grant no. CNS-1718130;

²All computations are on a laptop with an 11th Gen Intel(R) Core(TM) i5-11300H @ 3.10 GHz processor and 8 GB RAM, using a single core.

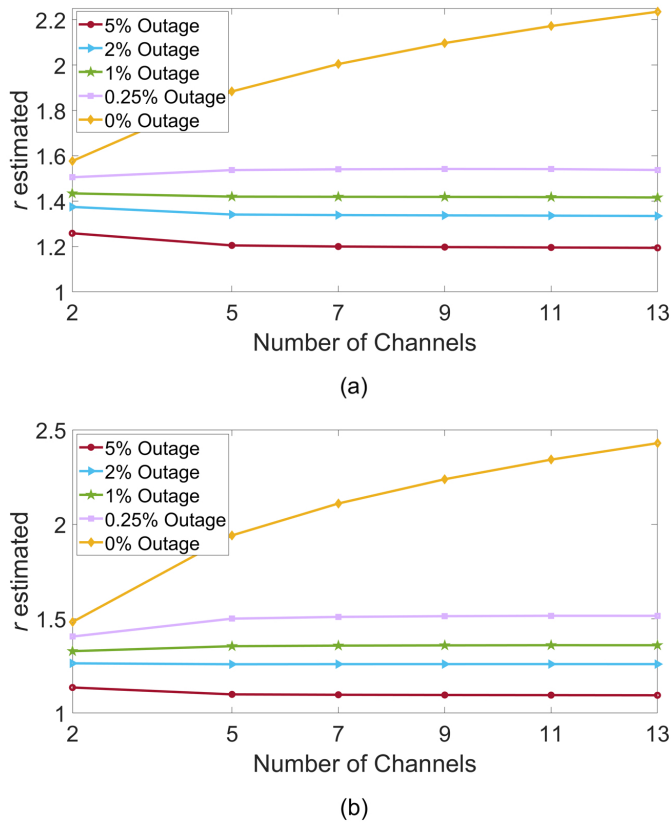


Fig. 3. Value of the PSGN parameter r needed to achieve a desired outage probability as the number of demands sharing the link varies; all channels have uniformly distributed bandwidth over (a) 50 to 100 GHz or (b) 50 to 200 GHz. The channels' maximum bandwidths are separated by 12.5 GHz guard-bands.

Swedish Research Council (VR) under grant no. 2021-03709; Zhejiang Provincial Natural Science Foundation no. LQ23F050013.

Disclosures. The authors declare no conflicts of interest.

REFERENCES

- O. Gerstel, M. Jinno, A. Lord, and S. Yoo, "Elastic optical networking: A new dawn for the optical layer?" *IEEE Commun. Mag.* **50**, 12–20 (2012).
- Y. Pointurier, "Design of low-margin optical networks," *IEEE/OSA J. Opt. Commun. Netw.* **9**, A9–A17 (2017).
- C. Delezoide, K. Christodouloupoulos, A. Kretsis, N. Argyris, G. Kanakis, A. Sgambelluri, N. Sambo, P. Giardina, G. Bernini, D. Roccato, A. Percelsi, R. Morro, H. Avramopoulos, E. Varvarigos, P. Castoldi, P. Layec, and S. Bigo, "Marginless operation of optical networks," *J. Light. Technol.* **37**, 1698–1705 (2019).
- K. Christodouloupoulos, C. Delezoide, N. Sambo, A. Kretsis, I. Sartzetakis, A. Sgambelluri, N. Argyris, G. Kanakis, P. Giardina, G. Bernini, D. Roccato, A. Percelsi, R. Morro, H. Avramopoulos, P. Castoldi, P. Layec, and S. Bigo, "Toward efficient, reliable, and autonomous optical networks: the ORCHESTRA solution," *J. Opt. Commun. Netw.* **11**, C10–C24 (2019).
- B. C. Chatterjee, N. Sarma, and E. Oki, "Routing and spectrum allocation in elastic optical networks: A tutorial," *IEEE Commun. Surv. Tuts.* **17**, 1776–1800 (2015).
- Y. Xu, E. Agrell, and M. Brandt-Pearce, "Probabilistic spectrum Gaus-

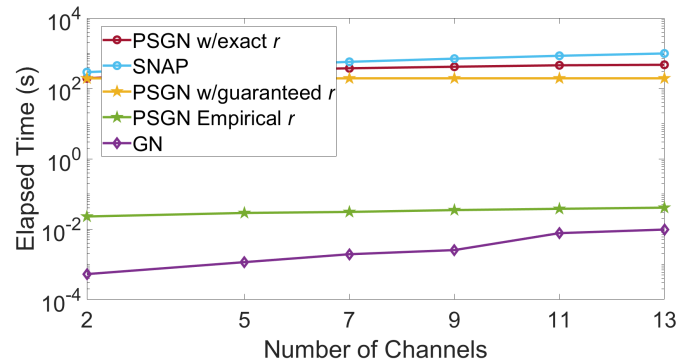


Fig. 4. Elapsed time in seconds for NLI estimation using various algorithms for different numbers of channels sharing the fiber link.

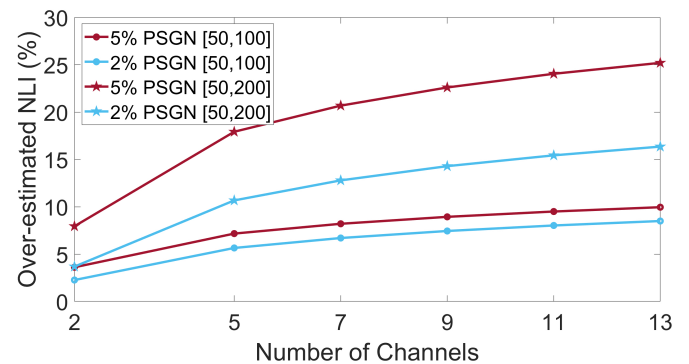


Fig. 5. NLI overestimation by the GN model over the PSGN model, calculated as $(G^{\text{GN}} - G^{\text{PSGN}}) / G^{\text{PSGN}}$. The channel of interest is the center channel suffering the most NLI.

sian noise estimate for random bandwidth traffic," in *Proc. European Conference on Optical Communication (ECOC)*, (2019).

- Y. Xu, E. Agrell, and M. Brandt-Pearce, "Static resource allocation for dynamic traffic," in *Proc. European Conference on Optical Communication (ECOC)*, (2019).
- M. Feknous, T. Houdoin, B. L. Guyader, J. D. Biasio, A. Gravey, and J. A. T. Gijón, "Internet traffic analysis: A case study from two major European operators," in *IEEE Symp. Comput. Commun. (ISCC)*, (2014).
- M. Klinkowski, M. Ruiz, L. Velasco, D. Careglio, V. Lopez, and J. Comellas, "Elastic spectrum allocation for time-varying traffic in flexgrid optical networks," *J. Sel. Areas Commun.* **31**, 26–38 (2013).
- M. Cantono, D. Pileri, A. Ferrari, C. Catanese, J. Thouras, J.-L. Augé, and V. Curri, "On the interplay of nonlinear interference generation with stimulated Raman scattering for QoT estimation," *J. Light. Technol.* **36**, 3131–3141 (2018).
- R. Dar, M. Feder, A. Mecozzi, and M. Shtaf, "Properties of nonlinear noise in long, dispersion-uncompensated fiber links," *Opt. Express* **21**, 25685–25699 (2013).
- P. Poggiolini and Y. Jiang, "Recent advances in the modeling of the impact of nonlinear fiber propagation effects on uncompensated coherent transmission systems," *J. Light. Technol.* **35**, 458–480 (2017).
- P. Johannisson and M. Karlsson, "Perturbation analysis of nonlinear propagation in a strongly dispersive optical communication system," *J. Light. Technol.* **31**, 1273–1282 (2013).
- H. Rabbani, H. Hosseinianfar, H. Rabbani, and M. Brandt-Pearce, "Analysis of nonlinear fiber Kerr effects for arbitrary modulation formats," *J. Light. Technol.* pp. 1–9 (2022).
- P. Poggiolini, G. Bosco, A. Carena, V. Curri, Y. Jiang, and F. Forghieri, "The GN-model of fiber non-linear propagation and its applications," *J.*

- Light. Technol. **32**, 694–721 (2014).
16. P. Johannisson and E. Agrell, "Modeling of nonlinear signal distortion in fiber-optic networks," *J. Light. Technol.* **32**, 4544–4552 (2014).
 17. M. Ranjbar Zefreh, F. Forghieri, S. Piciaccia, and P. Poggiolini, "Accurate closed-form real-time EGN model formula leveraging machine-learning over 8500 thoroughly randomized full C-Band systems," *J. Light. Technol.* **38**, 4987–4999 (2020).
 18. P. Serena and A. Bononi, "A time-domain extended Gaussian noise model," *J. Light. Technol.* **33**, 1459–1472 (2015).
 19. A. Carena, G. Bosco, V. Curri, Y. Jiang, P. Poggiolini, and F. Forghieri, "EGN model of non-linear fiber propagation," *Opt. Express* **22**, 16335–16362 (2014).
 20. M. Cantono, R. Gaudino, and V. Curri, "Potentialities and criticalities of flexible-rate transponders in DWDM networks: A statistical approach," *J. Opt. Commun. Netw.* pp. A76–A85 (2016).
 21. L. Yan, Y. Xu, M. Brandt-Pearce, N. Dharmaweera, and E. Agrell, "Robust regenerator allocation in nonlinear flexible-grid optical networks with time-varying data rates," *J. Opt. Commun. Netw.* pp. 823–831 (2018).
 22. V. Curri, M. Cantono, and R. Gaudino, "Elastic all-optical networks: A new paradigm enabled by the physical layer. How to optimize network performances?" *J. Light. Technol.* **35**, 1211–1221 (2017).
 23. B. Mukherjee, "WDM optical communication networks: progress and challenges," *J. Sel. Areas Commun.* **18**, 1810–1824 (2000).
 24. J. H. Lee, W. J. Lee, and N. Park, "Comparative study on temperature-dependent multichannel gain and noise figure distortion for 1.48- and 0.98- μm pumped EDFAs," *IEEE Photonics Technol. Lett.* **10**, 1721–1723 (1998).
 25. S. Y. Park, H. K. Kim, G. Y. Lyu, S. M. Kang, and S.-Y. Shin, "Dynamic gain and output power control in a gain-flattened erbium-doped fiber amplifier," *IEEE Photonics Technol. Lett.* **10**, 787–789 (1998).
 26. L. Yan, E. Agrell, H. Wymeersch, P. Johannisson, R. Di Taranto, and M. Brandt-Pearce, "Link-level resource allocation for flexible-grid nonlinear fiber-optic communication systems," *IEEE Photon. Technol. Lett.* **27**, 1250–1253 (2015).
 27. M. Hadi, M. R. Pakravan, and E. Agrell, "Dynamic resource allocation in metro elastic optical networks using Lyapunov drift optimization," *J. Opt. Commun. Netw.* **11**, 250–259 (2019).
 28. C. Chen, F. Zhou, M. Tornatore, and S. Xiao, "Maximizing revenue with adaptive modulation and multiple FECs in flexible optical networks," *IEEE/ACM Transactions on Netw.* **31**, 220–233 (2023).
 29. M. Rosenblatt, "Remarks on some nonparametric estimates of a density function," *The Annals Math. Stat.* **27**, 832 – 837 (1956).
 30. G. R. Terrell and D. W. Scott, "Variable kernel density estimation," *The Annals Stat.* pp. 1236–1265 (1992).
 31. R. Ramaswami and K. Sivarajan, "Routing and wavelength assignment in all-optical networks," *IEEE/ACM Transactions on Netw.* **3**, 489–500 (1995).
 32. P. S. Khodashenas, J. M. Rivas-Moscoco, D. Siracusa, F. Pederzoli, B. Shariati, D. Klonidis, E. Salvadori, and I. Tomkos, "Comparison of spectral and spatial super-channel allocation schemes for SDM networks," *J. Light. Technol.* **34**, 2710–2716 (2016).
 33. Y. Xu, E. Agrell, and M. Brandt-Pearce, "Cross-layer static resource provisioning for dynamic traffic in flexible grid optical networks," *J. Opt. Commun. Netw.* **13**, 1–13 (2021).